Video Article

High-resolution Thermal Micro-imaging Using Europium Chelate Luminescent Coatings

Timothy M. Benseman[1,2,3], Yang Hao[1,2], Vitalii K. Vlasko-Vlasov[1], Ulrich Welp[1], Alexei E. Koshelev[1], Wai-Kwong Kwok[1], Ralu Divan[4], Courtney Keiser[5], Chiharu Watanabe[6], Kazuo Kadowaki[6]

[1]Materials Science Division, Argonne National Laboratory

[2]Department of Physics, University of Illinois at Chicago

[3]Department of Physics, CUNY Queens College

[4]Center for Nanoscale Materials, Argonne National Laboratory

[5]Department of Physics, University of Northern Iowa

[6]Institute for Materials Science, University of Tsukuba

Correspondence to: Timothy M. Benseman at tbenseman@anl.gov

URL: https://www.jove.com/video/53948
DOI: doi:10.3791/53948

Keywords: Engineering, Issue 122, optical microscopy, fluorescence, semiconductor, cryogenics, high-temperature superconductivity, self-heating, europium chelate

Date Published: 4/16/2017

Citation: Benseman, T.M., Hao, Y., Vlasko-Vlasov, V.K., Welp, U., Koshelev, A.E., Kwok, W.K., Divan, R., Keiser, C., Watanabe, C., Kadowaki, K. High-resolution Thermal Micro-imaging Using Europium Chelate Luminescent Coatings. *J. Vis. Exp.* (122), e53948, doi:10.3791/53948 (2017).

Abstract

Micro-electronic devices often undergo significant self-heating when biased to their typical operating conditions. This paper describes a convenient optical micro-imaging technique which can be used to map and quantify such behavior. Europium thenoyltrifluoroacetonate (EuTFC) has a 612 nm luminescence line whose activation efficiency drops strongly with increasing temperature, due to *T*-dependent interactions between the Eu^{3+} ion and the organic chelating compound. This material may be readily coated on to a sample surface by thermal sublimation in vacuum. When the coating is excited with ultraviolet light (337 nm) an optical micro-image of the 612 nm luminescent response can be converted directly into a map of the sample surface temperature. This technique offers spatial resolution limited only by the microscope optics (about 1 micron) and time resolution limited by the speed of the camera employed. It offers the additional advantages of only requiring comparatively simple and non-specialized equipment, and giving a quantitative probe of sample temperature.

Video Link

The video component of this article can be found at https://www.jove.com/video/53948/

Introduction

Many electronic devices undergo strong self-heating when electrically biased to their normal operating conditions. This is usually due to a combination of low thermal conductivity (such as in semiconductors) and high power dissipation density. Furthermore, in devices with a semiconducting-like electrical resistivity (*i.e.* with $\partial\rho/\partial T < 0$) it has long been known that there exists the possibility of localized thermal runaway under certain biasing conditions [1,2], in which the bias current flows not uniformly through the device, but rather in narrow filaments which are associated with highly localized self-heating, typically on a scale of microns.

Understanding such self-heating physics may in some cases be essential for optimizing the design of a particular device, meaning that techniques for imaging temperature on micron scales are very useful. There has been a recent resurgence of interest in such techniques from two areas of technology development. The first of these is for imaging quench processes in high-temperature superconducting tapes in which thermal micro-imaging allows quench nucleation sites to be identified and studied [3,4]. The second application is for understanding self-heating in stacked intrinsic Josephson junction terahertz sources, which are fabricated from $Bi_2Sr_2CaCu_2O_8$. These have the combination of low thermal conductivity and semiconductor-like electrical conductivity along the relevant direction of current flow (*i.e.* their crystalline *c*-axis) described above. Not only do they experimentally show complex inhomogeneous self-heating behavior [5,6,7,8,9,10,11] it has been theoretically predicted that this may be beneficial for THz power emission [12,13].

A number of techniques exist for imaging the temperature of a sample at microscopic length scales. The thermoluminescent technique described here was originally employed for semiconducting devices near room temperature [14,15,16] but has more recently been applied at cryogenic bath temperatures to the superconducting tapes and THz sources described above [3,4,10,11]. Improvements in the resolution and signal-to-noise performance of CCD cameras have enabled considerable performance improvements in this technique over the last few decades. The Eu-coordination complex europium thenoyltrifluoroacetonate (EuTFC) has an optical luminescence which is strongly temperature dependent. The organic ligands in this complex effectively absorb UV light in a broad band around 345 nm. The energy is transferred radiation-less via intra-molecular excitations to the Eu^{3+} ion, which returns the complex to its ground state through the emission of a luminescence photon at 612 nm.

The strong temperature dependence arises from the energy transfer process [17] making for a sensitive thermal probe of an object coated with this material. When the coating is excited with a near-ultraviolet source — such as an Hg short-arc lamp — regions with lower luminescence intensity correspond to higher local temperature. The resulting images are limited in spatial resolution by the resolution of the microscope optics and the wavelength of the luminescence (in practice, to around 1 micron). Depending on the signal-to-noise ratio required, time resolution is limited only by the shutter speed of the camera, and more fundamentally by the decay time of the luminescence (no more than 500 µs) [15]. These characteristics make the technique a very fast probe of device temperature, which yields direct temperature measurements, using comparatively simple and economical equipment.

Variations of this technique published in the past by other groups have employed small concentrations of Eu-chelates dissolved in polymer films and spin-coated on to the sample surface [3,4]. This results in a coating which is highly uniform locally, but which has significant thickness variations at steps in the sample topography — such as commonly occur in microdevices — resulting in strong spatial variations in the luminescent response which can give artifacts in the images. The technique variation which we describe here employs thermal sublimation in vacuum. Not only does this avoid the macroscopic film thickness variation problem, but the higher EuTFC concentration achieved per unit area significantly improves the sensitivity and reduces the image acquisition time. A related technique employs a coating of SiC granules on the surface instead of the EuTFC [7,8,9]. SiC offers temperature sensitivity comparable to the EuTFC coatings described here, but the size of the granules limits the smoothness and resolution of the resulting images.

Several other techniques exist, which offer different combinations of advantages and disadvantages. Direct infrared imaging of blackbody radiation from the sample is simple and has spatial resolution of a few microns, but is only effective when the sample is significantly above room temperature. Scanning probe thermal microscopy techniques (such as scanning thermocouple microscopy or Kelvin probe microscopy) offer excellent sensitivity and spatial resolution, but have slow image acquisition times, necessarily limited by the scanning speed of the tip, as well as requiring highly complex equipment. Scanning laser or scanning electron beam thermal microscopy measures the voltage perturbation when a modulated beam is rastered across the surface of a current-biased device [6,7,18]. This offers excellent sensitivity, and is somewhat faster than scanning probe techniques, but once again requires highly complex equipment, and also gives an indirect, qualitative map of the sample temperature.

Protocol

1. Preparation of Sample for Coating

NOTE: If possible, remove all organic contamination from the surface of the sample to be thermally imaged. Any such contamination may react with the deposited EuTFC film and alter its luminescent response, causing position-dependent artifacts in the resulting thermal images. This is of particular importance with samples with Au surface electrodes, which tend to attract organic contamination from the atmosphere. Remove any particles or dust sitting on the sample surface at the same time, since these may result in artifacts also. The authors recommend the following procedure:

1. Make current and voltage connections to the devices on the sample such as superconducting bridges or resistive devices (*e.g.* wire bonds, painted-on connections using conductive epoxy, *etc.*) *before* cleaning it in preparation for thin film coating, as these steps may introduce contamination which should be removed before coating. Use Au wires if possible, since this will make it easier to connect the sample to the cryostat after the film has been deposited. (See step 4.6 below.)
2. Clean the sample in 100% acetone in an ultrasonic bath for 15 s.
3. Without allowing the sample to dry, clean it in 100% isopropyl alcohol in an ultrasonic bath for 5 s.
4. Blow the sample dry using a nitrogen gun.
5. If possible, clean any remaining organic residues off the sample surface using oxygen plasma ashing. To do this, use plasma power of 100 W, O_2 flow rate of 22 cm^3/s, and gas pressure of 160 mTorr, for 60 s. To avoid re-contamination of the sample, deposit the EuTFC coating as soon as possible after this step.

2. Preparation of Coating System for EuTFC Deposition

1. Use a sublimation source consisting of a purpose-built boat 20 x 10 x 10 mm^3 in size (l x w x h) made from stainless steel foil, enclosing a 10 coil of Manganin resistance wire, for operation at approximately 100 - 200 °C. Dissolve any melted-residues of EuTFC from the boat by soaking in acetone, as these will adversely affect the properties of the new film.
2. Rinse the boat in isopropyl alcohol.
3. Allow the boat to dry completely in air before proceeding to load EuTFC into it.
4. Protect EuTFC powder from water vapor and light while it is being stored. Thoroughly grind EuTFC powder using an agate mortar and pestle to remove any visible lumps.
   NOTE: Even when the powder is protected from water vapor, it may still crystallize into large lumps of 100 microns diameter or more. These must be removed as they will result in a grossly non-uniform film when sublimated, causing artifacts in the thermal images.
5. Install the sample holder and sublimation source in the vacuum coating system such that the sample sits approximately 10 mm directly above the source boat (suitably oriented crystal thickness sensor to monitor the deposition rate). Connect the source boat heater leads to their associated vacuum feedthroughs.
6. Fill the source boat approximately 2/3 full with approximately 0.2 g of ground EuTFC powder.
7. Mount the sample upside-down directly above the source boat (to ensure uniformity of the deposited film), preferably using double-sided tape or sticky dots, rather than vacuum grease which may contaminate the film.
8. To minimize exposure of the sample surface and the EuTFC powder to the atmosphere (especially water vapor) begin evacuation of the deposition chamber using a rotary pump as soon as possible.

3. Deposition of EuTFC Thin Film by Thermal Sublimation

1. Pump the deposition chamber to 3 x 10^{-5} mbar or less, preferably using a turbo-molecular pump.
2. Program the crystal thickness monitor to read for a film density of 1.50 g/cm^3.
3. Apply 0.5 W of power to the source boat heater, to gently warm the source until the EuTFC begins to sublimate. It will take 2 - 3 minutes for the thickness monitor to begin reading an appreciable deposition rate.
4. Adjust the heater power to maintain a deposition rate of 6 - 7 nm/minute. Make only small, slow adjustments, as the deposition rate typically takes 1 - 2 minutes to respond to changes in power input.
   NOTE: Boat temperatures sufficient to deposit more than 10 nm/minute in this configuration may cause the powder to melt in the boat, drastically reducing its surface area and thus the sublimation rate. More importantly, excessive boat temperatures may chemically alter the EuTFC and thus strongly reduce the thermal sensitivity of its luminescence.
5. After 200 nm (read by the thickness monitor) of film deposition, turn off the power to the source. (±20 nm is acceptable here, although thicknesses significantly outside this range will result in lower film sensitivity.)
6. After the reading on the thickness monitor reaches zero, vent the chamber, with dry nitrogen gas. After removal, protect the sample from light and water vapor as soon as possible, by storage in a light-proof container in a vacuum dessicator.
   NOTE: This will respectively prevent bleaching and chemical degradation of the EuTFC thin film.

4. Installation of Sample in Measurement Cryostat

1. Place a blob of vacuum grease on the center cryostat sample stage approximately 1-2 mm in diameter. Use a sample stage comprising a copper cold finger with a circular top surface 15 mm in diameter.
   NOTE: This is a sufficient size to ensure strong thermal contact between the stage and the sample when the sample is pressed down flat on top of it.
2. If the sample substrate is electrically conducting, isolate it from the stage by placing a 10 micron sheet of Mylar on top of the grease, and a second similarly sized blob on top of the Mylar.
   NOTE: The authors find that it is better to use grease with a comparatively high viscosity (*e.g.* silicone-based high vacuum grease) than specialized heat-sinking compounds, as the latter typically contain low-viscosity components which may flow on to the top surface of the sample and contaminate its EuTFC coating.
3. Press the sample down on top of the grease using tweezers to apply force to two diagonally opposite corners simultaneously, and then clamp in place at least two corners, using brass screws and BeCu clamps.
   NOTE: If the sample is not securely held in position, then it may drift significantly relative to the microscope when power is applied to it, making the resulting images difficult to analyze.
4. Make any necessary electrical connections such as for current and voltage leads from the sample to the cryostat wiring, taking care not to allow contamination (*e.g.* droplets of solder flux) to land on the EuTFC film.
   NOTE: Do this by using only the smallest amount of flux which will do the job, and preferably avoid using flux for this step at all. Flux should not be necessary if Au wires are used for the connections to the sample.
5. Mount the sample cryostat on its xyz translation stage underneath the microscope, install its heat shield and optical window, and evacuate its sample space with a turbomolecular pump.
6. Cover the optical window of the cryostat with a piece of aluminum foil (or similar) to prevent bleaching of the EuTFC by ambient lighting in the room. Take care not to damage or contaminate the microscope lens when doing this.
7. Cool the cryostat to the bath temperature of interest. For the samples described in this paper, this is typically between 5 K and 100 K.
   NOTE: Do not allow the sample stage to sit for prolonged periods of time at temperatures between 125 K and 175 K, since in this range the EuTFC film will eventually crystallize into a polygranular state with inhomogeneous luminescence properties which can also drift over time. Cooling through this temperature range at 2 K/minute or faster will ensure that this problem does not occur. If the cryostat is accidentally left in this temperature range for too long, the EuTFC film may be reproducibly 'reset' by simply warming the cryostat to at least 190 K for 5 minutes.

5. Collection of Thermal Image Data

1. Install a short-pass filter with 500 nm cut-off wavelength in the illumination optics path.
2. Install a band-pass filter with passband center wavelength = 610 nm, and FWHM = 10 nm, in the collection optics path.
   NOTE: A narrow passband is advantageous here, since it minimizes collection of background light which contributes to the noise, but not to the signal. The filters must also be chosen to minimize spectral crosstalk between them.
3. Allow the light source to warm up and stabilize at its steady-state operating temperature, and allow the camera to cool to its equilibrium operating temperature. This should take around 30 minutes in both cases.
4. With all optical filters in place (since the focus position is wavelength-dependent) illuminate the sample and align and focus the microscope to the region of interest.
   NOTE: While the sample is not being imaged, use a shutter or similar to avoid unnecessary illumination of the sample and resultant bleaching of the EuTFC film.
5. Collect a reference image with zero current applied to the sample. When collecting each image, make a correction for dark counts, which can vary strongly from pixel to pixel, as well as giving a significant offset to the true image counts from the luminescent signal.
   NOTE: The exposure conditions used will depend on the requirements of the experiment (see discussion) but it is important to choose the exposure conditions such that the image contains no saturated pixels. The reference image is needed since the collected luminescent intensity will typically vary strongly depending on the surface reflectivity of the sample, even when its temperature is entirely uniform.
6. Apply electrical bias to the sample, collect an image under the same exposure conditions as the reference, and compute the intensity ratio of these. NOTE: The level of electrical bias required depends strongly on the combination of device and self-heating behavior which are being studied. The examples presented here typically result from sample bias currents of the order of tens of mA, resulting in a few volts of bias across the device.

NOTE: If the sample has moved significantly relative to the reference image, then the pixel data should be shifted to compensate. (However, depending on the performance of the camera, this shift may introduce noise from pixel-to-pixel variations in its sensitivity to light, which is why movement of the sample should be minimized if at all possible.) If high absolute accuracy in temperature measurements is required, small drifts in the lamp intensity may be corrected for by normalizing the image-to-reference ratio to be 1 in a suitable region of the sample (*i.e.* one which is sufficiently far from the self-heated device as to be unaffected by it).

7. Repeat step 5.6 for all bias conditions of interest, while keeping the bath temperature constant.
8. Repeat steps 5.4 through to 5.7 for all bath temperatures of interest.
   NOTE: Depending on the cryostat, the sample may need to be realigned and refocused at each new bath temperature.

6. Calibration of Results

1. Collect zero-applied-current reference images sufficient to cover the entire temperature range of interest. 3 to 4 images at each temperature will suffice to establish reproducibility, while 20 K spacing will give enough data points to generate an accurate calibration curve. (See **Figure 1b**.)
2. From this curve, convert the normalized intensity images into temperature maps. While the absolute luminescent intensity depends strongly on the local surface reflectivity of the sample, its normalized behavior with respect to temperature is only very weakly affected by this.

7. Sample Storage and Film Re-use

1. As always, keep the film protected from bleaching by ambient light. NOTE: If necessary, the EuTFC coating on a sample can withstand repeated thermal cycling, and its properties will remain stable over a period of 2-3 weeks when kept in high vacuum.
   NOTE: However, even when stored in high vacuum at room temperature, the film will degrade over 2-3 months. (Discoloration and roughening of the film can be easily seen under an optical microscope.) If this occurs on a sample which requires additional thermal images, then clean the film off and replace it as per steps 1 to 3.

Representative Results

An example of a typical measurement configuration for conducting this experiment at cryogenic bath temperatures is shown in **Figure 1a**, while a typical curve of 612 nm luminescent response intensity versus temperature is plotted in **Figure 1b**.

Figure 2 shows an example of typical thermal images of self heating in a $Bi_2Sr_2CaCu_2O_8$ THz source, which consists of a 'mesa' of stacked 'intrinsic' Josephson junctions with dimensions 300 x 60 x 0.83 microns, fabricated on the surface of a single crystal, and having a superconducting T_c of 86 K.

In such a device, the current flow is along the *c*-axis direction (*i.e.* into the plane of the page as shown in the images) due to the extremely anisotropic electrical resistivity of this material. As shown in **Figure 2a**, ρ_c(T) for $Bi_2Sr_2CaCu_2O_8$ falls strongly with increasing temperature, allowing the possibility of thermal instabilities and localized thermal runaway under certain biasing conditions. Thermal images of the device are shown in **Figure 2d**, which were collected as described in the text under 160X magnification, using summed exposures of 4 x 2 s on a 1,024 x 1,024 pixel CCD camera with 16-bit resolution, Peltier-cooled to -50 °C. The sample was illuminated with a short-arc Hg lamp using a 500 nm short-pass filter, and net intensity of approximately 1 W/cm^2. To avoid the requirement of normalizing the images by an un-self-heated area as described in section 5.6, the lamp was operated using a variable iris with closed-loop feedback to keep illumination intensity constant over time.

The images reveal a localized hotspot, where local self-heating gives rise to self-sustaining filament of current flowing through the device in the *c*-axis direction. In this filament, the current density is over 5 times higher than in the rest of the mesa. The current-voltage characteristic for the mesa at T_{bath} = 25 K is shown in **Figure 2b**. This contains hysteretic jumps associated with the nucleation/annihilation of the hotspot at around I_{bias} = 11 mA, and with the jumping of the hotspot from the electrode end of the mesa to the opposite end between 40 and 60 mA. **Figure 2c** shows longitudinal cross-sections of the mesa surface temperature under different bias conditions. For the camera and imaging conditions used here, the temperature noise is around 0.2 K, when smoothed over a diameter of 4 microns, corresponding to a 5 x 5 pixel region at this magnification. The lines visible in **Figure 2d** at the edges of the mesa and of the electrode are artifacts due to reflection off near-vertical sidewall surfaces.

Figure 3 shows raw image examples of situations which should be avoided as described in the protocol. **Figure 3a** shows a 612 nm luminescent image in which the film was sublimated using EuTFC in which mm-sized lumps were present. (See step 2.4.) These sublimated violently when heated, depositing particles of EuTFC several microns in diameter on to the sample. **Figure 3b** shows a sample whose EuTFC coating has crystallized into domains after 16 hours at 150 K, resulting in uneven and noisy luminescent response. (See step 4.6.)

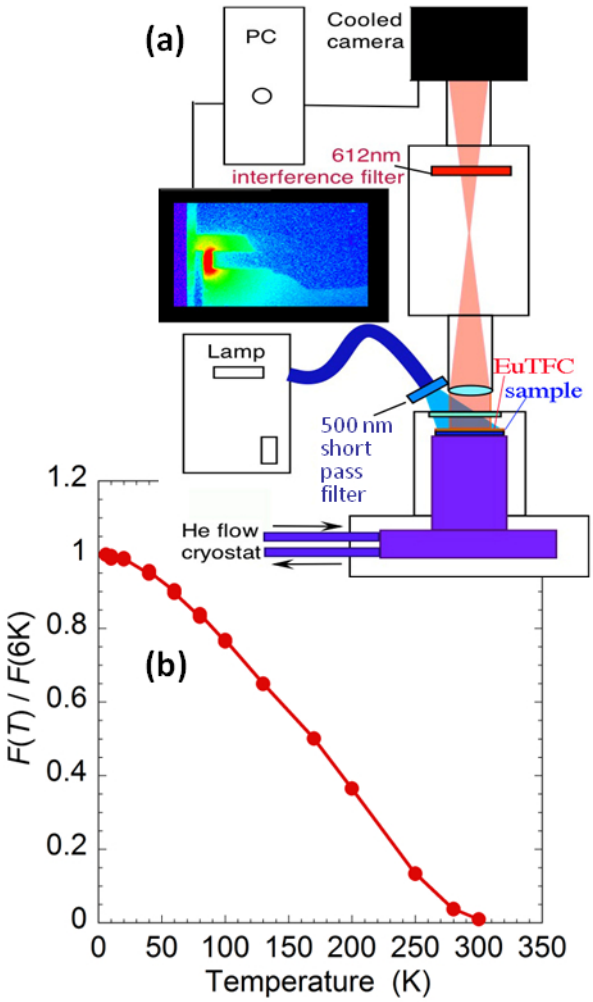

Figure 1: Thermal Imaging setup and typical calibration curve. (**a**) Configuration of Microscope, UV light source, and cryostat with optical window, modified from reference 10. (**b**) Response curve normalized to 10 K for 200 nm sublimated EuTFC film.

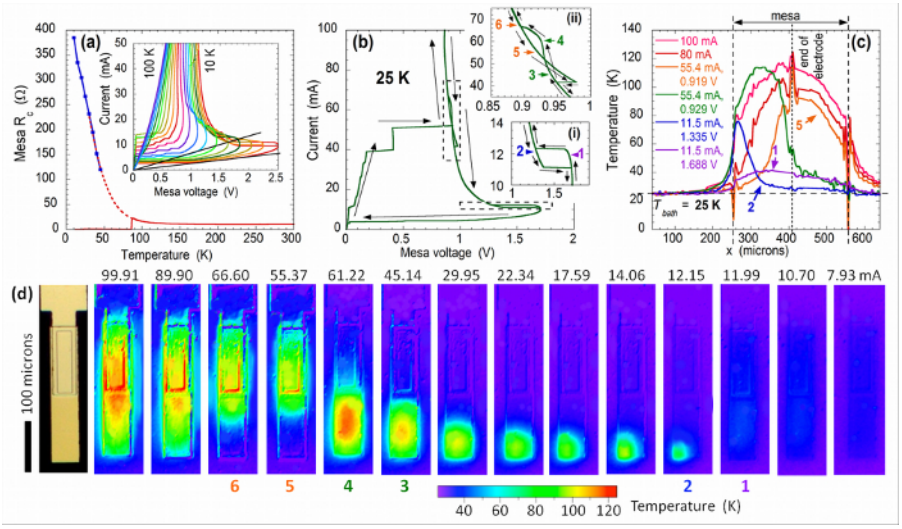

Figure 2: $Bi_2Sr_2CaCu_2O_8$ mesa THz source: I-V characteristics & thermal images. (**a**) (Main) Plot of device resistance against temperature. Blue squares plotted below T_c are values extrapolated from I-V curves shown in inset. (**b**) I-V characteristic showing hysteretic switching of Josephson junctions in device at T_{bath} = 25 K, for current-biased mesa. Insets (i) and (ii) show jumps in mesa resistance associated with hotspot nucleation and relocation respectively. (**c**) Longitudinal temperature cross-sections of mesa. (**d**) Thermal images at T_{bath} = 25 K, modified from reference 11, with conventional optical micrograph of mesa shown at left. Please click here to view a larger version of this figure.

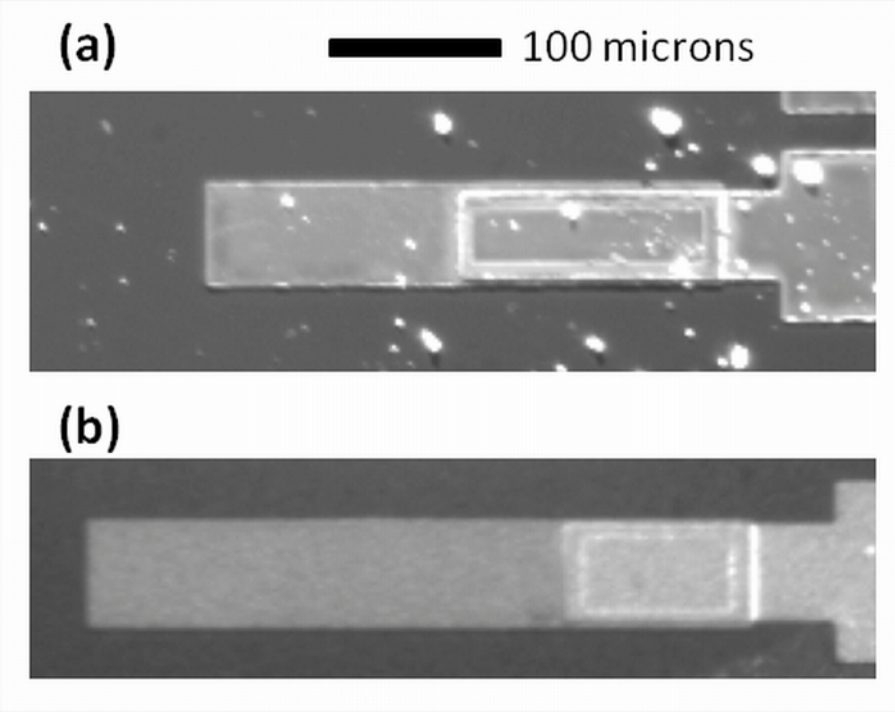

Figure 3: Examples of problems to avoid with EuTFC film. (**a**) Film sublimated without removing large crystallized lumps from EuTFC powder, resulting in lumps deposited on sample. (**b**) Film (deposited on a different mesa) which has undergone local crystallization after 16 hours in cryostat at 150 K, showing uneven luminescent response. Please click here to view a larger version of this figure.

Discussion

As demonstrated by our results, the technique described in this article yields high-resolution thermal images of microdevices, with good sensitivity and using only simple optical microscopy equipment. The advantages of this technique relative to alternative methods (which will be discussed below) are strongest at approximately 250 K and below, meaning that its most important applications are for studying the self-heating of devices which are designed to operate at cryogenic bath temperatures. These include superconducting current tapes (where quench nucleation is of key engineering interest), narrow band-gap semiconductors for optical detection, and novel high-T_c electronic devices whose resistance drops with increasing T.

If the technique is to work with optimum sensitivity, then it is critical to follow correct procedures for the deposition of the film. The sample surface must be cleaned thoroughly (protocol steps 1.1 to 1.5), the EuTFC powder must be carefully ground to remove any lumps which can adversely affect the uniformity of the film (step 2.4), and the film sublimation must occur at the correct rate in order to preserve the correct chelation of the Eu^{3+} ion (steps 3.3 and 3.4). Recrystallization of the film at cryogenic temperatures may increase the experimental noise level, but this problem can be reversed as described in step 4.7. The illumination and exposure parameters which should be used, and the resulting signal-to-noise, depend on the requirements of the experiment. Here we discuss some of the considerations which limit the performance of the technique.

There are four main possible contributions to the noise in this experiment, namely photon shot noise, microscopic variation in the luminescent response of the film, variations in camera pixel sensitivity, and camera dark count shot noise. Where I is the excitation illuminance (in incident photons per unit of pixel-equivalent sample area), $F(T)$ is the T-dependent overall luminescent conversion efficiency for each pixel-equivalent area of the film (which is affected by the local film thickness), S is the CCD count yield from a pixel per incident photon (at = 612 nm), and D is the number of dark counts collected over exposure time t, then when averaged over P pixels, these parameters will be approximately normally distributed as follows:

$$I \sim N\left(\bar{I},\ \sqrt{\bar{I}/P}\right)$$
$$F(T) \sim N\left(\bar{F}(T),\ \sigma_F(T)/\sqrt{P}\right)$$
$$S \sim N\left(\bar{S},\ \sigma_S/\sqrt{P}\right)$$
$$D \sim N\left(\bar{D}Pt,\ \sigma_D\sqrt{Pt}\right)$$

$\sigma_F(T)$ depends on the uniformity of the EuTFC coating, while the standard deviation σ_S in pixel-to-pixel light sensitivity and dark count rate standard deviation σ_D depend on the performance of the camera. The counts collected over P pixels for time t therefore have mean:

$$\langle Counts \rangle = \bar{I}\bar{F}(T)\bar{S}Pt + \bar{D}Pt$$

where the last term corresponds to the dark count contribution, and variance:

$$\sigma_{Counts}^2 = \begin{bmatrix} \bar{I}^2\bar{F}(T)^2\sigma_z^2/P + \bar{I}^2\bar{S}^2\sigma_F^2(T)/P + \bar{I}\bar{F}(T)^2\bar{S}^2/P \\ + \bar{I}^2\sigma_F^2(T)\sigma_z^2/P^2 + \bar{I}\bar{F}(T)^2\sigma_z^2/P^2 + \bar{I}\bar{S}^2\sigma_F^2(T)/P^2 \\ + \bar{I}\sigma_F^2(T)\sigma_z^2/P^3 \end{bmatrix} P^2t + \sigma_D^2Pt$$

Therefore the standard error in the measured temperature when averaged over P pixels with total exposure time t is given by:

$$\sigma_T = \frac{\sigma_{Counts}}{\langle Counts\rangle - \langle Dark\ Counts\rangle} \times \frac{1}{\bar{F}(T)}\frac{d\bar{F}(T)}{dT}$$
$$= \frac{\sqrt{\begin{bmatrix} \bar{I}^2\bar{F}(T)^2\sigma_z^2/P + \bar{I}^2\bar{S}^2\sigma_F^2(T)/P + \bar{I}\bar{F}(T)^2\bar{S}^2/P \\ + \bar{I}^2\sigma_F^2(T)\sigma_z^2/P^2 + \bar{I}\bar{F}(T)^2\sigma_z^2/P^2 + \bar{I}\bar{S}^2\sigma_F^2(T)/P^2 \\ + \bar{I}\sigma_F^2(T)\sigma_z^2/P^3 \end{bmatrix} P^2t + \sigma_D^2Pt}}{\bar{I}\bar{F}(T)\bar{S}Pt} \times \frac{d}{dT}\left[\ln \bar{F}(T)\right]$$

For a highly uniform film and a CCD with low pixel response non-uniformity , the terms in $\sigma_F(T)$ and σ_S respectively may usually be neglected. The temperature error thus simplifies to:

$$\sigma_T = \frac{\sqrt{\left[\bar{I}\bar{F}(T)^2\bar{S}^2/P\right]P^2t + \sigma_D^2Pt}}{\bar{I}\bar{F}(T)\bar{S}Pt} \times \frac{d}{dT}\left[\ln \bar{F}(T)\right]$$
$$= \frac{\sqrt{\bar{I}\bar{F}(T)^2\bar{S}^2 + \sigma_D^2}}{\bar{I}\bar{F}(T)\bar{S}\sqrt{Pt}} \times \frac{d}{dT}\left[\ln \bar{F}(T)\right]$$

For the conditions normally employed in this technique, the rate of luminescent photon collection is of the order of 5000 photons per pixel per second. For a modern cooled CCD camera, the rate of dark counts and thus σ_D is significantly less than this, meaning that σ_T is usually limited by photon shot noise [19]. If σ_D can be neglected, then the temperature error simplifies further to:

$$\sigma_T = \frac{1}{\sqrt{\bar{I}Pt}} \times \frac{d}{dT}\left[\ln \bar{F}(T)\right]$$

Increasing the illumination intensity thus reduces the exposure time required for any given σ_T, especially in exceptional cases where the luminescent yield is low (*e.g.* at temperatures close to 300 K), and where dark counts are in fact significant. However, intense UV illumination may photodope carriers into semiconducting samples, and break Cooper pairs in superconducting ones, thereby perturbing the properties of the device being studied. In samples whose surfaces have a weak thermal path to the cold bath, strong illumination may also introduce a heat load which causes a significant rise in the sample temperature.

All of these considerations may sometimes necessitate low illumination intensities and longer exposure times. As a modification, shorter exposures may be required to image fast phenomena such as current filament oscillation or breathing modes [20], or the millisecond timescales of quench development in superconductors. Where high signal-to-noise ratios in absolute temperature measurements are required, then longer total exposure times are called for. This may require summation of multiple exposures, depending on the bit resolution of the CCD electronics. Image-intensified cameras have close to single-photon detection efficiency, and offer a more attractive trade-off between image noise, illumination intensity, averaging area, and exposure speed, albeit at higher system cost.

In summary, the thermoluminescent imaging technique which we describe here offers a direct quantitative measure of sample surface temperature, with high temporal and spatial resolution. It is also effective at a wide range of temperatures, from 5 K to over 300 K. As described in the Introduction, alternative techniques exist, but each of these offers a combination of advantages and disadvantages.

Scanning probe techniques offer excellent sensitivity, at the cost of long measurement times and highly specialized equipment. A recently-published pyro-magneto-optical technique also offers excellent sensitivity [21]. However, this technique relies on a ferrimagnetic garnet indicator crystal placed on top of the sample, which limits spatial resolution, especially where the sample is not topographically flat. At temperatures above 300 K, the luminescent yield from EuTFC becomes low, and direct imaging of infrared blackbody radiation from the sample becomes a more effective technique.

Disclosures

The authors have nothing to disclose.

Acknowledgements

Work at Argonne National Laboratory was funded by the Department of Energy, Office of Basic Energy Sciences, under Contract No. DE-AC02-06CH11357, which also funds Argonne's Center for Nanoscale Materials (CNM) where the patterning of the BSCCO mesa was performed. We thank R. Divan and L. Ocola for their help with sample fabrication.

References

1. Ridley, B. K., Specific Negative Resistance in Solids. *Proc. Phys. Soc.* **82**, 954 - 966 (1963).
2. Lueder, H., & Spenke, E., Über den Einfluß der Wärmeableitung auf das elektrische Verhalten von temperaturabhängigen Widerständen. *Physikalische Zeitschrift.* **36**, 767 - 773 (1935).
3. Haugen, O., *et al.*, High Resolution Thermal Imaging of Hotspots in Superconducting Films. *IEEE Trans. Appl. Supercond.* **17**, 3215 - 3218 (2007).
4. Niratisairak, S., Haugen, O., Johansen, T. H., & Ishibashi, T., Observation of hotspot in BSCCO thin film structure by fluorescent thermal imaging. *Physica C.* **468**, 442 (2008).
5. Wang, H. B., *et al.*, Hot Spots and Waves in $Bi_2Sr_2CaCu_2O_8$ Intrinsic Josephson Junction Stacks: A Study by Low Temperature Scanning Laser Microscopy. *Phys. Rev. Lett.* **102**, 017006 (2009).
6. Wang, H. B., *et al.*, Coherent Terahertz Emission of Intrinsic Josephson Junction Stacks in the Hot Spot Regime. *Phys. Rev. Lett.* **105**, 057002 (2010).
7. Minami, H., *et al.*, Local SiC photoluminescence evidence of hot spot formation and sub-THz coherent emission from a rectangular $Bi_2Sr_2CaCu_2O_{8+\delta}$ mesa. *Phys. Rev. B.* **89**, 054503 (2014).
8. Watanabe, C., Minami, H., Yamamoto, T., Kashiwagi, T., Klemm, R. A., & Kadowaki, K., Spectral investigation of hot spot and cavity resonance effects on the terahertz radiation from high-T_c superconducting $Bi_2Sr_2CaCu_2O_{8+\delta}$ mesas. *J. Phys.: Condens. Matter.* **26**, 172201 (2014).
9. Tsujimoto, M., Kambara, H., Maeda, Y., Yoshioka, Y., Nakagawa, Y., & Kakeya, I. Dynamic Control of Temperature Distributions in Stacks of Intrinsic Josephson Junctions in $Bi_2Sr_2CaCu_2O_{8+\delta}$ for Intense Terahertz Radiation. *Phys. Rev. Applied.* **2**, 044016 (2014).
10. Benseman, T. M., *et al.*, Direct imaging of hot spots in $Bi_2Sr_2CaCu_2O_{8+\delta}$ mesa terahertz sources. *J. Appl. Phys.* **113**, 133902 (2013).
11. Benseman, T. M., *et al.*,Current filamentation in large $Bi_2Sr_2CaCu_2O_{8+\delta}$ mesa devices observed via luminescent and scanning laser thermal microscopy. *Phys. Rev. Applied.* **3** 044017 (2015).
12. Koshelev, A. E., & Bulaevskii, L. N., Resonant electromagnetic emission from intrinsic Josephson-junction stacks with laterally modulated Josephson critical current. *Phys. Rev. B.* **77**, 014530 (2008).
13. Koshelev, A. E., Alternating dynamic state self-generated by internal resonance in stacks of intrinsic Josephson junctions. *Phys. Rev. B.* **78**, 174509 (2008).
14. Kolodner, P., & Tyson, J. A., Microscopic fluorescent imaging of surface temperature profiles with 0.01 °C resolution. *Appl. Phys. Lett.* **40**, 782 - 784 (1982).
15. Kolodner, P., & Tyson, J. A., Remote thermal imaging with 0.7-μm spatial resolution using temperature-dependent fluorescent thin films. *Appl. Phys. Lett.* **42**, 117 - 119 (1983).
16. Hampel, G., High power failure of superconducting microwave filters: Investigation by means of thermal imaging. *Appl. Phys. Lett.* **69**, 571 - 573 (1996).
17. Hadjichristov, G. B., Stanimirov, S. S. Stefanov, I. L & Petkov, I. K., The luminescence response of diamine-liganded europium complexes upon resonant and pre-resonant excitation. *Spectrochimica Acta A.* **69**, 443 - 448 (2008).
18. Mayer, B., Doderer, T., Huebener, R. P., & Ustinov A. V., Imaging of one- and two-dimensional Fiske modes in Josephson tunnel junctions. *Phys. Rev. B.* **44**, 12463 - 12473 (1991).
19. See for instance *http://hamamatsu.magnet.fsu.edu/articles/ccdsnr.html.* (2016).
20. Niedernostheide, F. J., Kerner, B. S., & Purwins, H.-G., Spontaneous appearance of rocking localized current filaments in a nonequilibrium distributive system. *Phys. Rev. B.* **46**, 7559 (1992).
21. Kustov, M., Grechishkin, R., Gusev, M., Gasanov, O., & McCord, J., Thermal Imaging: A Novel Scheme of Thermographic Microimaging Using Pyro-Magneto-Optical Indicator Films. *Advanced Materials.* **27**, 4950 (2015).

